J|A|C|S
ARTICLES
Published on Web 08/10/2004

Relaxation-Optimized NMR Spectroscopy of Methylene Groups in Proteins and Nucleic Acids

Emeric Miclet, David C. Williams Jr., G. Marius Clore, David L. Bryce, Jérôme Boisbouvier,*,† and Ad Bax*

Contribution from the Laboratory of Chemical Physics, National Institute of Diabetes and Digestive and Kidney Diseases, National Institutes of Health, Bethesda, Maryland 20892-0520

Received April 12, 2004; E-mail: jerome.boisbouvier@ibs.fr; bax@nih.gov

Abstract: A large fraction of hydrogens in proteins and nucleic acids is of the methylene type. Their detailed study, however, in terms of structure and dynamics by NMR spectroscopy is hampered by their fast relaxation properties, which give rise to low sensitivity and resolution. It is demonstrated that six different relaxation interference processes, involving $^1H-^{13}C$ and $^1H-^1H$ dipolar interactions and ^1H and ^{13}C chemical shift anisotropy, can be used simultaneously to mitigate these problems effectively. The approach is applicable to the majority of NMR experiments commonly used to study side chain and backbone conformation. For proteins, its efficiency is evaluated quantitatively for two samples: the third IgG-binding domain from Streptococcal Protein G and the protein calmodulin complexed with a 26-residue target peptide. Gains in both resolution and sensitivity by up to factors of 3.2 and 2.0, respectively, are observed for Gly residues at high magnetic field strengths, but even at much lower fields gains remain substantial. The resolution enhancement obtained for methylene groups makes possible a detailed analysis of spectral regions commonly considered inaccessible due to spectral crowding. For DNA, the high resolution now obtainable for C_5' sites permits an H_5'/H_5''-based sequential NOE assignment procedure, complementary to the conventional base-$H_1'/H_2'/H_2''$ pathway.

Introduction

In recent years, it has been shown that transverse-relaxation-optimized NMR spectroscopy (TROSY) methods can extend the application of NMR to considerably larger systems. To date, TROSY experiments have been described for optimizing observation of $^{15}N-^1H$ amide groups,[1,2] aromatic $^{13}C-^1H$ sites,[3−5] and most recently $^{13}C-^1H_3$ methyl groups.[6] No such methods have been available for methylene groups, even though they represent 46% of the observable protons in proteins, and the C_5' methylene group in nucleic acids represents a critical backbone element. Frequently, these methylene regions are difficult to access due to severe spectral crowding.

Here we present an approach, based on relaxation-optimized spectroscopy and multiplet simplification, that considerably improves both the resolution and sensitivity of methylene group NMR studies. The approach is applicable both to small molecules, where it is primarily the suppression of geminal $^1H-^1H$ splittings that enhances spectral appearance, and biological macromolecules, where the benefits of the improved relaxation properties selected in our experiments further enhance spectral quality. Conceptually, the new approach is an extension of earlier E.COSY based technology,[7] aimed at measurement of $^1H-^{13}C$ and $^1H-^1H$ dipolar couplings in protein[8] and nucleic acid[9] methylene groups. The element introduced here for optimized NMR observation of methylene groups can be incorporated in many of today's most common 2D and 3D NMR experiments. As an example, we show its incorporation in 3D ^{13}C-separated NOESY, enabling observation of the sequential $H_5'-H_1'$ NOEs in DNA and thereby providing sequential assignment information. The experiments also provide access to the measurement of the geminal $^1H-^1H$ scalar and dipolar coupling, as well as both corresponding one-bond $^1H-^{13}C$ interactions.

Methods

All NMR experiments were carried out on Bruker DRX spectrometers, operating at ^1H frequencies of 500 or 800 MHz and equipped respectively with a cryogenic (500 MHz) or a regular (800 MHz) triple resonance pulsed field gradient probehead, optimized for ^1H detection.

† Present address: Laboratoire de RMN, Institut de Biologie Structurale, Jean-Pierre Ebel, UMR 5075 CNRS-CEA-UJF, 41 rue Jules Horowitz, 38027 GRENOBLE Cedex 1, France.

(1) Pervushin, K.; Riek, R.; Wider, G.; Wuthrich, K. *Proc. Natl. Acad. Sci. U.S.A.* **1997**, *94*, 12366−12371.
(2) Riek, R.; Wider, G.; Pervushin, K.; Wuthrich, K. *Proc. Natl. Acad. Sci. U.S.A.* **1999**, *96*, 4918−4923.
(3) Pervushin, K.; Riek, R.; Wider, G.; Wuthrich, K. *J. Am. Chem. Soc.* **1998**, *120*, 6394−6400.
(4) Brutscher, B.; Boisbouvier, J.; Pardi, A.; Marion, D.; Simorre, J. P. *J. Am. Chem. Soc.* **1998**, *120*, 11845−11851.
(5) Fiala, R.; Czernek, J.; Sklenar, V. *J. Biomol. NMR* **2000**, *16*, 291−302.
(6) Tugarinov, V.; Hwang, P. M.; Ollerenshaw, J. E.; Kay, L. E. *J. Am. Chem. Soc.* **2003**, *125*, 10420−10428.
(7) Griesinger, C.; Sørensen, O. W.; Ernst, R. R. *J. Chem. Phys.* **1986**, *85*, 6837−6852.
(8) Carlomagno, T.; Peti, W.; Griesinger, C. *J. Biomol. NMR* **2000**, *17*, 99−109.
(9) Miclet, E.; O'Neil-Cabello, E.; Nikonowicz, E. P.; Live, D.; Bax, A. *J. Am. Chem. Soc.* **2003**, *125*, 15740−15741.

All data sets have been processed with nmrPipe.[10] For resolution and sensitivity comparisons, no apodization of the time domain data was employed. Data were zero-filled by a factor of 2 in all dimensions prior to Fourier transformation.

Three different samples were employed. The first sample comprised 1.8 mM uniformly (>95%) ^{13}C,^{15}N-labeled third IgG-binding domain from Streptococcal Protein G, hereafter referred to as GB3, dissolved in D_2O, pH 5.6, 50 mM sodium phosphate (data were acquired at 10 °C). The second protein sample contained 1 mM uniformly (>95%) ^{13}C,^{15}N-enriched calmodulin, complexed with an unlabeled 26-residue peptide comprising the calmodulin-binding domain of skeletal muscle myosin light chain kinase, hereafter referred to as CaM/M13,[11] dissolved in D_2O, pH 6.8, 100 mM KCl (data acquired at 35 °C). The third sample corresponds to a 19-base-pair DNA binding site of the transcription factors Oct-1 and Sox-2 in the HoxB1 promoter.[12] One strand (purchased from Silantes GmbH, Munich, Germany) is uniformly ^{13}C,^{15}N-enriched (5′-TGTCTTTGTCATGCTAATG-3′) and forms a duplex with the unlabeled complementary DNA strand (5′-CATTAG-CATGACAAAGACA-3′). The DNA duplex was dissolved in D_2O, at a concentration of 0.8 mM, in 10 mM sodium phosphate, 10 mM dithiothreitol, and 0.02% NaN_3, pH 6.5 (data acquired at 35 °C).

Quantum chemical calculations of methylene proton chemical shielding tensors were carried out using the GIAO method as implemented in Gaussian03,[13] the hybrid B3LYP functional, and the 6-311++G(3df,3pd) basis set on all atoms. Results reported are for the methylene group of the model system $H_3C-N(H)-C(O)-CH_2-N(H)-CH_3$, which was constructed using standard bond lengths and angles, a N−C′−C^{α}−N dihedral angle (psi) of 135°, and a C′−C^{α}−N−C^{Me} dihedral angle of −139°, to mimic a glycine residue in an antiparallel beta strand geometry. Calculations of the absolute chemical shielding tensors for Gly-$^1H^{\alpha}$ methylene protons yield the following parameters: for the $H^{\alpha 2}$ proton (pro-R), $\sigma_{xx} = 23.0$ ppm, $\sigma_{yy} = 28.3$ ppm, $\sigma_{zz} = 30.4$ ppm; angles between the C−H vector and these three principal components are equal to 82.6°, 7.4°, 89.5°, and angles between the H−H vector and these three principal components are equal to 47.3°, 42.8°, 89.7°. For the $H^{\alpha 3}$ proton (pro-S), the principal components are $\sigma_{xx} = 23.9$ ppm, $\sigma_{yy} = 27.9$ ppm, $\sigma_{zz} = 33.6$ ppm; angles between the C−H vector and these three principal components are equal to 82.7°, 73.7°, 18.0°; and angles between the H−H vector and these three principal components are equal to 49.8°, 67.0°, 49.0°. Calculations at the same level of theory on tetramethylsilane (B3LYP/6-311+G* optimized structure) yield a proton isotropic chemical shielding of 31.6 ppm.

Theoretical Section

We consider a system of three coupled spin-$^1/_2$ nuclei (^{13}C, $^1H^1$, and $^1H^2$), corresponding to an isolated methylene group. Each spin is assumed to be characterized by an axially symmetric chemical shielding tensor. The single quantum NMR spectrum of each proton consists of a doublet of doublets, corresponding to the different spin states of the other ^1H and the ^{13}C. Each of the four components of proton H^1 (Figure 1a) can be described by a single-transition operator (H^{PQ}), which can be represented as a combination of product operator terms,[14] describing in-phase and antiphase transverse

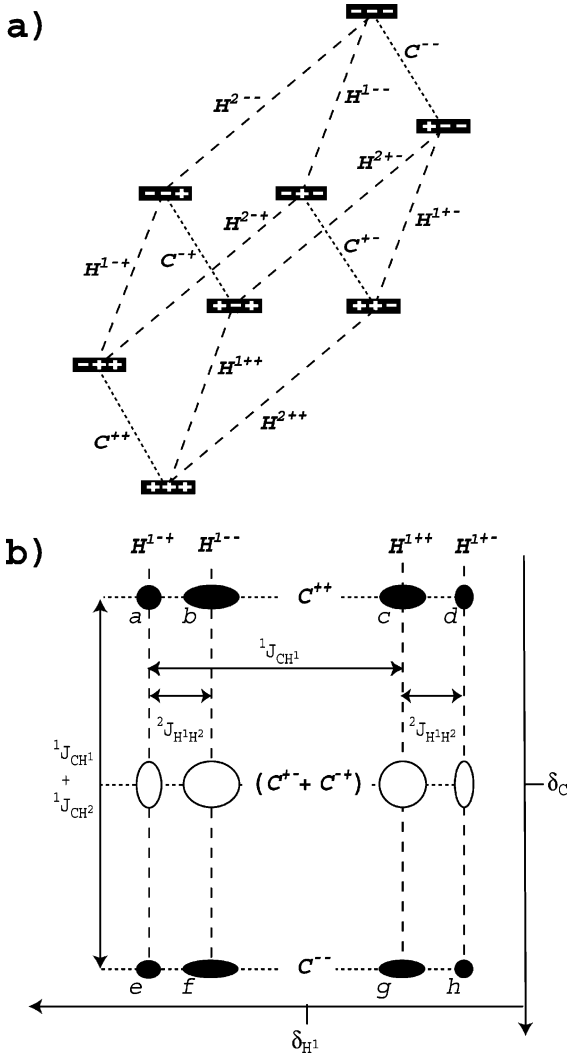

Figure 1. NMR transitions in a $^{13}CH_2$ group. (a) Energy level diagram of an isolated CH^1H^2 spin system. Each eigenstate is defined by three signs "+" or "−" (with "+" for $m_z = +^1/_2$ and "−" for $m_z = -^1/_2$), where the first sign corresponds to the ^{13}C spin state and the two latter signs to H^1 and H^2. Long-dashed lines depict ^1H transitions, and short-dashed lines are ^{13}C transitions, each labeled with its single transition operator, defined in eqs 1 and 3. (b) Schematic representation of the 2D multiplet pattern observed for an individual methylene ^1H in a fully coupled HSQC experiment. The diagram corresponds to $^1J_{CH} > 0$, $^2J_{HH} < 0$ and $^1J_{CH^1} = {}^1J_{CH^2} \gg |^2J_{H^1H^2}|$. For $^1J_{CH^1} = {}^1J_{CH^2}$, C^{-+} and C^{+-} transitions have vanishing intensity (open ellipsoids). The chemical shift frequencies are marked δ_C and δ_H. Horizontal short-dashed lines and vertical long-dashed lines mark ^{13}C and ^1H frequency transitions, respectively. The transverse relaxation rate for each transition is defined in eqs 2, 4, and 5. Italic characters *a*−*h* correspond to the panels of Figure 4 which display this multiplet component experimentally.

coherences H_x^1, $2H_x^1C_z$, $2H_x^1H_z^2$, $4H_x^1C_zH_z^2$:

$$H^{PQ} = H_x^1 + p \times 2H_x^1C_z + q \times 2H_x^1H_z^2 + pq \times 4H_x^1C_zH_z^2 \quad (1)$$

where P and Q characterize the eigenstates of C_z and H_z^2 respectively: $(P,Q) \in \{(+,+);(+,-);(-,+);(-,-)\}$, with "+" and "−" corresponding to $m_z = +^1/_2$ ($|\alpha\rangle$ spin state) and $m_z = -^1/_2$ ($|\beta\rangle$ spin state), respectively. Correspondingly, $p = 1$ for $P = +$; $p = -1$ for $P = -$; $q = 1$ for $Q = +$; $q = -1$ for $Q = -$. With the relative magnitude and the sign of couplings involved in a methylene spin system taken into account, the position of each multiplet component, corresponding to an

(10) Delaglio, F.; Grzesiek, S.; Vuister, G. W.; Zhu, G.; Pfeifer, J.; Bax, A. *J. Biomol. NMR* **1995**, *6*, 277−293.
(11) Ikura, M.; Clore, G. M.; Gronenborn, A. M.; Zhu, G.; Klee, C. B.; Bax, A. *Science* **1992**, *256*, 632−638.
(12) Williams, D. C.; Cai, M. L.; Clore, G. M. *J. Biol. Chem.* **2004**, *279*, 1449−1457.
(13) Frisch, M. J.; Trucks, G. W.; Schlegel, H. B.; Scuseria, G. E.; Pople, J. A., et al. *Gaussian 03*, revision B.04; Gaussian Inc.: Pittsburgh, PA, 2003.
(14) Sørensen, O. W.; Eich, G. W.; Levitt, M. H.; Bodenhausen, G.; Ernst, R. R. *Prog. Nucl. Magn. Reson. Spectrosc.* **1983**, *16*, 163−192.

individual ^{1}H transition, is indicated in Figure 1b. As a result of interference between the different dipole−dipole and chemical shift anistropy (CSA) relaxation mechanisms operating on a given ^{1}H, different line widths are expected for each multiplet component. The relaxation rate of an individual transition is described by[15]

$$R(H^{PQ}) = \Gamma^{DD,DD}_{H^1C,H^1C} + \Gamma^{DD,DD}_{H^1H^2,H^1H^2} + \Gamma^{CSA,CSA}_{H^1,H^1} - p \times \Gamma^{CSA,DD}_{H^1,H^1C} - q \times \Gamma^{CSA,DD}_{H^1,H^1H^2} + pq \times \Gamma^{DD,DD}_{H^1C,H^1H^2} \quad (2)$$

where the first three terms correspond to dipolar ($\Gamma^{DD,DD}_{H^1C,H^1C}$, $\Gamma^{DD,DD}_{H^1H^2,H^1H^2}$) and CSA ($\Gamma^{CSA,CSA}_{H^1,H^1}$) autorelaxation rates, and the last three terms correspond to cross-correlated relaxation between H^1 CSA and H^1−C dipole−dipole interaction ($\Gamma^{CSA,DD}_{H^1,H^1C}$), H^1 CSA and H^1−H^2 dipole−dipole interaction ($\Gamma^{CSA,DD}_{H^1,H^1H^2}$), and dipole−dipole cross-correlated relaxation between H^1−C and H^1−H^2 ($\Gamma^{DD,DD}_{H^1C,H^1H^2}$). The four single-transition operators and corresponding relaxation rates for proton H^2 are obtained by interchanging indices 1 and 2 in eqs 1 and 2.

The four ^{13}C transitions (Figure 1a) are described by

$$C^{PQ} = C_x + p \times 2C_xH^1_z + q \times 2C_xH^2_z + pq \times 4C_xH^1_zH^2_z \quad (3)$$

where P and Q now represent the eigenstates of H^1_z and H^2_z, respectively. In a ^{1}H-coupled HSQC spectrum of a methylene group, the two center components of the doublet-of-doublets, corresponding to transitions C^{+-} and C^{-+}, are of opposite phase and cancel one another. The spectrum then appears as a doublet in the ^{13}C dimension, consisting of the two observable transitions C^{++} and C^{--}, separated by $^1J_{CH^1} + {}^1J_{CH^2}$. Analogous to eq 2, the relaxation rates of the ^{13}C multiplet components are described by

$$R(C^{PQ}) = \Gamma^{DD,DD}_{CH^1,CH^1} + \Gamma^{DD,DD}_{CH^2,CH^2} + \Gamma^{CSA,CSA}_{C,C} - p \times \Gamma^{CSA,DD}_{C,CH^1} - q \times \Gamma^{CSA,DD}_{C,CH^2} + pq \times \Gamma^{DD,DD}_{CH^1,CH^2} \quad (4)$$

Assuming isotropic rotational diffusion in the slow tumbling limit for a macromolecule with fast internal dynamics of moderate amplitude, the individual auto- and cross-correlated relaxation rates (eqs 2 and 4) are given by[15]

$$\Gamma^{DD,DD}_{HC,HC} = \Gamma^{DD,DD}_{CH,CH} = (\xi^{DD}_{HC})^2\tau_C\mathbf{S}^2/5 \quad (5a)$$

$$\Gamma^{DD,DD}_{H^1H^2,H^1H^2} = (\xi^{DD}_{H^1H^2})^2\tau_C\mathbf{S}^2/4 \quad (5b)$$

$$\Gamma^{CSA,CSA}_{A,A} = 4(\xi^{CSA}_{A})^2\tau_C\mathbf{S}^2/45 \quad (5c)$$

$$\Gamma^{CSA,DD}_{A,AM} = 4\xi^{CSA}_{A}\,\xi^{DD}_{AM}P_2(\cos\theta^{CSA,DD}_{A,AM})\tau_C\mathbf{S}^2/15 \quad (5d)$$

$$\Gamma^{DD,DD}_{AM,AX} = 2\xi^{DD}_{AM}\,\xi^{DD}_{AX}P_2(\cos\theta^{DD,DD}_{AM,AX})\tau_C\mathbf{S}^2/5 \quad (5e)$$

where A, M, and X denote the C, H^1, or H^2 spins, in arbitrary order, $\xi^{DD}_{AM} = (\mu_o h\gamma_A\gamma_M/8\pi^2)\langle r^{-3}_{AM}\rangle$, $\xi^{CSA}_{A} = \gamma_A B_0\Delta\sigma_A$, $\theta^{\mu,\mu'}$ is the angle between the principal axis of interactions μ and μ', τ_c is the global correlation time, r_{AM} is the distance between nuclei A and M, and $\mathbf{S}^2$ is the squared generalized order parameter.[16] Although, strictly speaking, a specific order parameter should be introduced for each pair of correlated interactions, in this study we assume a uniform value of $\mathbf{S}^2 = 0.8$, frequently a reasonable approximation.[17] The symbol $\Delta\sigma_A$ denotes the chemical shielding anisotropy of spin A, defined as $\Delta\sigma_A = (\sigma_{11} - (\sigma_{22} + \sigma_{33})/2)$, where σ_{11} is the chemical shielding tensor component furthest from the isotropic shielding value.

Results and Discussion

As described in the theoretical section, the fully coupled (in both ^{1}H and ^{13}C dimensions) HSQC spectrum will show eight multiplet components for each methylene proton of an isolated $^{13}CH_2$ group. The different coefficients applicable for each multiplet component when calculating the total relaxation rate from the sum of the autorelaxation and cross correlation terms of eqs 2−5, $\Gamma^{CSA,DD}_{H^1,H^1C}$, $\Gamma^{CSA,DD}_{H^1,H1H^2}$, $\Gamma^{DD,DD}_{H^1C,H^1H^2}$, $\Gamma^{CSA,DD}_{C,CH^1}$, $\Gamma^{CSA,DD}_{C,CH^2}$, and $\Gamma^{DD,DD}_{CH^1,CH^2}$, result in different line widths for each of these eight components, schematically indicated in Figure 1b. Analogous to the well-known ^{1}H−^{15}N TROSY experiment,[1] selection of the slowest relaxing component will enhance spectral resolution. As described below, such a selection can be made with high efficiency by a suitably optimized pulse scheme, yielding considerable resolution enhancement and even increases in sensitivity over conventional HSQC experiments. Below, the experiment is quantitatively analyzed for the three-spin system of Gly residues in uniformly ^{13}C-enriched proteins, dissolved in D_2O. Application to other methylene spin systems in biomacromolecules, outside of the isolated-three-spin approximation, will also be presented.

Methylene Spin-State-Selective Correlation. Figure 2a shows the implementation of a 2D experiment that specifically selects one of the eight methylene HSQC multiplet components. This 2D CH_2-TROSY pulse scheme is very similar to the standard inverse heteronuclear two-dimensional sensitivity-enhanced HSQC experiment[18] but lacks ^{1}H decoupling during t_1 and ^{13}C decoupling during t_2. It also uses modified timing durations in the final "Rance−Kay" element of the pulse sequence to accomplish $^{13}CH_2$ spin-state-selective coherence transfer or CH_2-S^3CT.

The pulse scheme starts with an initial INEPT transfer of ^{1}H magnetization to ^{13}C (time point *a*). An S^3E element,[19,20] between time points *a* and *b*, then selects the slowest relaxing, most downfield component of the ^{13}C multiplet, C^{--}. The total S^3E duration, normally $1/(4^1J_{CH})$ for methine ^{13}C−^{1}H groups, is reduced to $1/(8^1J_{CH}) \approx 880$ μs, to account for the 2^1J_{CH} separation between the outer multiplet components in the ^{13}C dimension. The C^{++} magnetization component is eliminated by the 90° ^{13}C pulse applied at time point *b*, which rotates it to the *z*-axis, whereas the C^{--} magnetization remains in the transverse plane and evolves during t_1 with frequency $\delta_C + {}^1J_{CH}$. This magnetization is then encoded by gradients G_4 and G_5. As pointed out above, C^{--} can be written as the sum of the four product operator terms: $C^{--} = C_x - 2C_xH^1_z - 2C_xH^2_z + 4C_xH^1_zH^2_z$. The subsequent methylene spin-state-selective coherence transfer (point *d* to *e* in Figure 2a) transforms C^{--} into the following four ^{1}H single quantum coherences: H^1_x,

(15) Kumar, A.; Grace, R. C. R.; Madhu, P. K. *Prog. Nucl. Magn. Reson. Spectrosc.* **2000**, *37*, 191−319.
(16) Lipari, G.; Szabo, A. *J. Am. Chem. Soc.* **1982**, *104*, 4546−4559.
(17) Tjandra, N.; Bax, A. *Science* **1997**, *278*, 1111−1114.
(18) Kay, L. E.; Keifer, P.; Saarinen, T. *J. Am. Chem. Soc.* **1992**, *114*, 10663−10665.
(19) Meissner, A.; Duus, J. O.; Sorensen, O. W. *J. Magn. Reson.* **1997**, *128*, 92−97.
(20) Meissner, A.; Duus, J. O.; Sorensen, O. W. *J. Biomol. NMR* **1997**, *10*, 89−94.

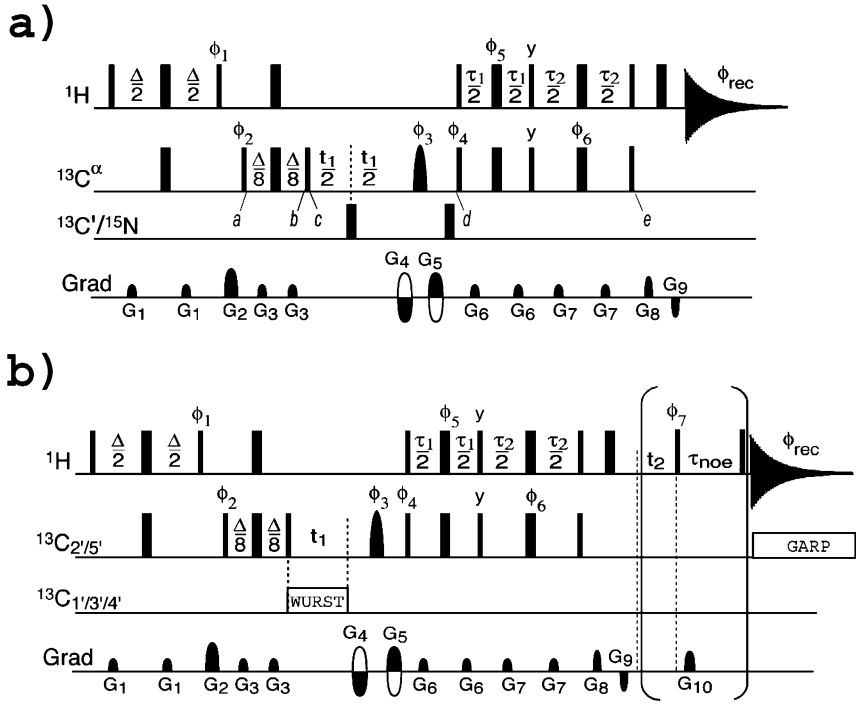

Figure 2. Pulse schemes of CH_2-TROSY experiments. Narrow and wide bars indicate nonselective 90° and 180° pulses, respectively. Unless specified, pulse phases are *x*. Delay durations: $\Delta = 1/(2J_{CH})$; $\tau_1 = 0.34/(J_{CH})$; $\tau_2 = 0.23/(J_{CH})$. For selection of the downfield, C^{--} components: $\phi_1 = -y$; $\phi_2 = (225°, 45°)$; $\phi_5 = x$; and $\phi_6 = x$ are used to select the H^{+-} component in the ^{1}H dimension (see Table 1); $\phi_3 = (x,x,y,y)$, $\phi_4 = x$ and $\phi_{rec} = (x,-x,-x,x)$. The experiment is recorded in the regular Rance−Kay manner:[18] for each t_1 increment, two FID's are acquired, one with G_4, G_5, and ϕ_4 inverted, and stored separately. Field gradients are sine-bell shaped with durations $G_{1,...,10}$ of 1, 2, 0.25, 1, 1, 0.2, 0.3, 0.35, 0.153, 0.6 ms; amplitudes of 10, 18, 12, 30, 30, 10, 12, 30, 30, 18 G/cm; and directions *x*, *xy*, *y*, −*z*, *z*, *x*, *y*, *z*, −*z*, *xyz*. (a) 2D CH_2-TROSY experiment, in the nonconstant-time mode (i.e., optimal for Gly). The shaped $^{13}C^{\alpha}$ pulse has a REBURP profile (3.1 ms duration at 800 MHz for a 6 ppm bandwidth inversion). $^{13}C'$ 180° pulses (carrier at 177 ppm) are sine-bell-shaped and have durations of 180 μs. (b) Pulse scheme of the 2D CH_2-TROSY and 3D CH_2-TROSY-NOESY adapted for nucleic acids. The shaped $^{13}C'_{2/5}$ pulse has been generated by coadding two REBURP profiles,[21] designed to refocus selectively two separate frequency regions: 65−70 ppm and 38−43 ppm (3.75 ms pulse duration at 800 MHz). Homonuclear band-selective $^{13}C'_{1,3,4}$ effective decoupling over the 76−89 ppm frequency range is achieved by means of a train of 180° adiabatic pulses (WURST-4 created with the Bruker shape tool, Q_0 factor = 4, for an inversion bandwidth of ±1300 Hz, maximum radio frequency field strength $\gamma B_1/2\pi = 804$ Hz, 5.25 ms duration at 800 MHz)[22] in a p5m4 composite decoupling sequence {2 × (0, 150, 60, 150, 0), 2 × (180, 330, 240, 330, 180)}.[23] ^{13}C decoupling during acquisition is only applied for the 3D experiments, using a GARP decoupling sequence with $\gamma B_1/2\pi = 4.2$ kHz. Quadrature detection in ^{13}C (t_1) and ^1H (t_2) dimension is achieved by recording four separate free induction decays or FIDs (E_1 to E_4) per pair of (t_1,t_2) values, with the following phases and gradient settings: $E_1 = \{\phi_4 = x, \phi_7 = x, G_4, G_5\}$; $E_2 = \{\phi_4 = -x, \phi_7 = x, -G_4, -G_5\}$; $E_3 = \{\phi_4 = x, \phi_7 = y, G_4, G_5\}$; and $E_4 = \{\phi_4 = -x, \phi_7 = y, -G_4, -G_5\}$. Prior to Fourier transformation, the FIDs are rearranged as follows: $E_1' = \{E_1 + E_2\}$; $E_2' = \{E_4 - E_3\}$; $E_3' = \{E_3 + E_4\}$; and $E_4' = \{E_1 - E_2\}$. Corresponding Bruker pulse programs and NMRpipe macros are available at http://spin.niddk.nih.gov/bax/.

$2H_x^1C_z$, $-2H_x^1H_z^2$, $-4H_x^1C_zH_z^2$. With identical values assumed for the two one-bond couplings, $^1J_{CH^1} = {}^1J_{CH^2} = J_{CH}$, the transfer efficiency in this CH_2-S^3CT element is the same for generation of $H_x^1(\tau_1, \tau_2)$ and $-4H_x^1C_zH_z^2(\tau_1, \tau_2)$ terms and described by a factor $f(\tau_1, \tau_2)$:

$$f(\tau_1, \tau_2) = \cos(\pi J_{CH}\tau_1)\sin(\pi J_{CH}\tau_2) + \sin(\pi J_{CH}\tau_1) \quad (6a)$$

Generation of $2H_x^1C_z(\tau_1, \tau_2)$ and $-2H_x^1H_z^2(\tau_1, \tau_2)$ also carries a common prefactor:

$$g(\tau_1, \tau_2) = \sin(\pi J_{CH}\tau_1)\cos(\pi J_{CH}\tau_1)\cos(\pi J_{CH}\tau_2) + \cos(\pi J_{CH}\tau_2)\sin(\pi J_{CH}\tau_2)[1 + \sin^2(\pi J_{CH}\tau_1)] \quad (6b)$$

If τ_1 and τ_2 delays are chosen such that $f(\tau_1, \tau_2) = g(\tau_1, \tau_2)$, cancellation occurs for signals corresponding to transitions H^{++}, H^{--}, and H^{-+} (Figure 3a). In contrast, the terms contributing to H^{+-} magnetization add constructively, yielding a ^{1}H multiplet in which only the most upfield component has nonzero intensity (Figure 3a). Although a continuous range of (τ_1, τ_2) values can satisfy $f(\tau_1, \tau_2) = g(\tau_1, \tau_2)$ (Figure 3b), the solution ($\tau_1 = 0.34/{}^1J_{CH}$; $\tau_2 = 0.23/{}^1J_{CH}$) corresponds to the highest transfer efficiency (Supporting Information Figure S1), and use of these values maximizes the sensitivity of correlating C^{--} and H^{+-} transitions.

Figure 4 demonstrates that each of the eight $^1H-^{13}C$ multiplet components for a given methylene proton can be selected separately with the pulse scheme of Figure 2a. The correlations correspond to the $C^{\alpha}H^{\alpha 3}$ spin pair of Gly-41 in GB3. Different correlations in the ^{1}H dimension are selected by changing phases ϕ_5 and ϕ_6 in the CH_2-S^3CT element in the manner described in Table 1. These phases control the signs of the (τ_1, τ_2)-dependent transverse ^{1}H magnetization terms, generated by the CH_2-S^3CT element: $H_x^1(\tau_1, \tau_2)$, $4H_x^1C_zH_z^2(\tau_1, \tau_2)$, $2H_x^1C_z(\tau_1, \tau_2)$, and $2H_x^1H_z^2(\tau_1, \tau_2)$. So, these terms can be individually inverted, without affecting their absolute magnitude. Next to selection of the desired proton transition by ϕ_5 and ϕ_6, the phase ϕ_2 of the ^{13}C 90° pulse preceding the S^3E element controls selection of the desired ^{13}C multiplet component, evolving during t_1. Analogous to previously proposed TROSY experiments for $^{15}N-^1H$ and aromatic $^{13}C-^1H$ spin systems,[4,24] the

(21) Geen, H.; Freeman, R. *J. Magn. Reson.* **1991**, *93*, 93−141.
(22) Kupce, E.; Freeman, R. *J. Magn. Reson., Ser. A* **1996**, *118*, 299−303.
(23) Fujiwara, T.; Nagayama, K. *J. Magn. Reson.* **1988**, *77*, 53−63.

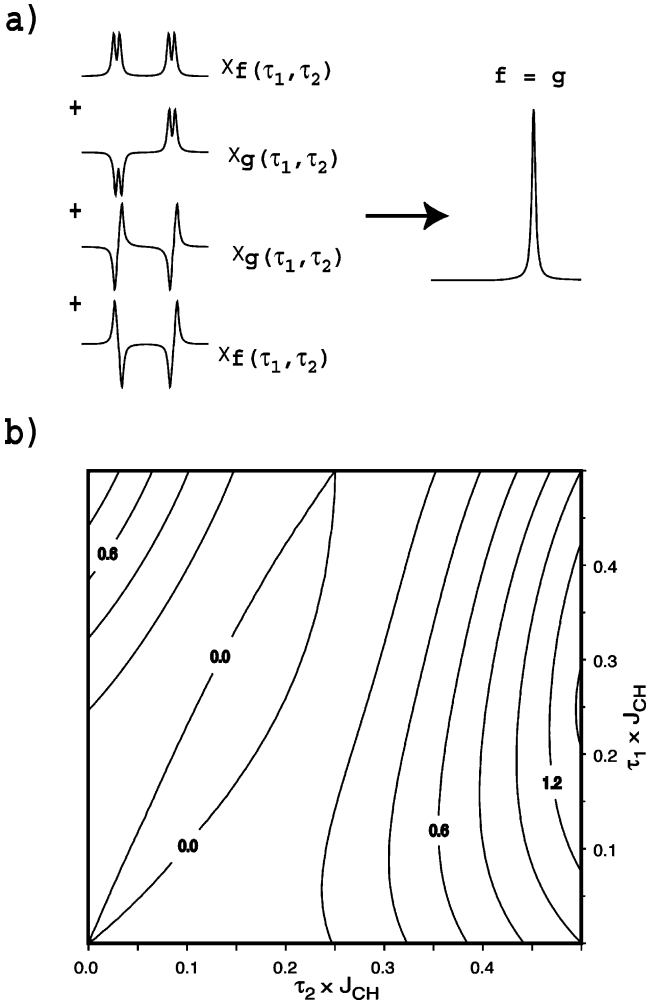

Figure 3. Selection of individual multiplet components in CH_2-TROSY. (a) Schematic representation of ^1H resonances corresponding to in-phase and antiphase terms (i) H_x, (ii) $2H_xC_z$, (iii) $-2H_xH_z$, and (iv) $-4H_xC_zH_z$, generated after the CH_2 spin-state selective coherence transfer. The magnitudes of the (i) and (iv) terms are proportionate to the function $f(\tau_1, \tau_2)$; (ii) and (iii) are proportionate to $g(\tau_1, \tau_2)$, with $f(\tau_1, \tau_2) = \cos(\pi J_{CH}\tau_1)\sin(\pi J_{CH}\tau_2) + \sin(\pi J_{CH}\tau_1)$ and $g(\tau_1, \tau_2) = \sin(\pi J_{CH}\tau_1)\cos(\pi J_{CH}\tau_1)\cos(\pi J_{CH}\tau_2) + \cos(\pi J_{CH}\tau_2)\sin(\pi J_{CH}\tau_2)(1 + \sin^2(\pi J_{CH}\tau_1))$. For $f(\tau_1, \tau_2) = g(\tau_1, \tau_2)$, only one ^1H multiplet component remains when coadding the spectra. (b) Contour plot of $f(\tau_1, \tau_2) - g(\tau_1, \tau_2)$.

Table 1. Phase Settings in Figure 2 for Selection of Each of the Eight Components of a CH_2 Group[a]

transition selected		ϕ_1[a]	ϕ_2[a]	ϕ_5[a]	ϕ_6[a]	component[b]
C^{++}	H^{+-}	y	135°/315°	y	x	d
	H^{++}	y	135°/315°	x	y	c
	H^{--}	y	135°/315°	y	y	b
	H^{-+}	y	135°/315°	x	x	a
C^{--}	$\boldsymbol{H^{+-}}$	$\boldsymbol{-y}$	**225°/45°**	$\boldsymbol{x}$	$\boldsymbol{x}$	**h**
	H^{++}	$-y$	225°/45°	y	y	g
	H^{--}	$-y$	225°/45°	x	y	f
	H^{-+}	$-y$	225°/45°	y	x	e

[a] Bold entries correspond to selection of the narrowest component, i.e., to the CH_2-TROSY experiment. [b] The character corresponds to the Figure 4 panel containing this multiplet component.

steady-state Boltzmann ^{13}C polarization can be added to the magnetization transferred from ^1H by appropriate selection of the phase ϕ_1 in Figure 2, thereby enhancing sensitivity. For each of the eight multiplet components, the optimized combinations of radio frequency phases are given in Table 1.

Incomplete suppression of multiplet components not selected by a given combination of phases in Table 1 can arise from deviations from the $\tau_1 = 0.34/^1J_{CH}$ and $\tau_2 = 0.23/^1J_{CH}$ condition, which cannot be met simultaneously for the experimental range of $^1J_{CH}$ values (referred to as $^1J_{CH}$ mismatching).[25,26] Other causes of incomplete suppression include differential relaxation,[27,28] the finite lifetime of the passive spin state,[29] and, in particular for the methylene case, evolution resulting from the relatively large $^2J_{HH}$ coupling. The selection efficiency of the S^3E element in the presence of $^1J_{CH}$ mismatching has already been well documented.[26,30] Simulation[31] of effects induced by the neglected $^2J_{HH}$ evolution or due to $^1J_{CH}$ mismatch during the CH_2-S^3CT element demonstrate that the intensity of multiplet components not selected by any given phase cycle combination of Table 1 will be ≤0.6% (for $^2J_{HH} = -18$ Hz) and ≤1% (for $\Delta^1J_{CH}/^1J_{CH} \leq 0.1$). Because the transfer delays τ_1 and τ_2 are relatively short, the effect of passive spin state flips or differential relaxation during the final CH_2-S^3CT element is relatively small and does not result in significant breakthrough of unselected components. Perhaps surprisingly, initial experiments using 500-μL sample volumes in regular NMR tubes revealed that B_1-field inhomogeneity can result in detectable spurious peaks (up to 4% of the selected component). However, in all tested cases (using 500 and 600 MHz cryogenic probeheads and 600 and 800 MHz room-temperature probes), this artifact is reduced below 1% by restricting the sample height, using a 280-μL volume in a thin-wall Shigemi microcell. One-dimensional cross sections, shown in Figure 4, confirm that no selection artifacts are observable at the noise threshold. However, accurate pulse calibrations remain critical to achieve clean selection: simulated and experimental results indicate that ^1H or ^{13}C pulse miscalibration by as little as 5% can result in selection artifacts of up to 7%.

Whereas, in standard ^1H-coupled HSQC experiments, correlations involving the C^{-+} and C^{+-} transitions are not observed, they can potentially lead to undesirable correlations in the CH_2-TROSY experiment. It can be shown that such artifacts arise from the ^{13}C Boltzmann polarization (vide infra, eq 8). In this case, the CH_2-S^3CT element converts the C^{-+} and C^{+-} coherences into the $H^{++} - H^{--}$ combination of single-transition operators, with an efficiency that depends on delays τ_1 and τ_2 (data not shown). To study this artifact more precisely, CH_2-TROSY spectra with enhanced intensity of this artifact were recorded for the GB3 sample by starting from in-phase ^{13}C magnetization. The undesired signal at the ^{13}C chemical shift frequency, δ_C, then consists of a doublet, antiphase in the ^1H dimension and separated by $^1J_{CH} + {}^2J_{HH}$, in agreement with theoretical analysis (data not shown). Calculations for $\tau_1 = 0.34/^1J_{CH}$ and $\tau_2 = 0.23/^1J_{CH}$ indicate that the intensity of this artifact

(24) Pervushin, K. V.; Wider, G.; Wuthrich, K. *J. Biomol. NMR* **1998**, *12*, 345−348.
(25) Meissner, A.; Schulte-Herbruggen, T.; Briand, J.; Sorensen, O. W. *Mol. Phys.* **1998**, *95*, 1137−1142.
(26) Sorensen, M. D.; Meissner, A.; Sorensen, O. W. *J. Biomol. NMR* **1997**, *10*, 181−186.
(27) Rance, M.; Loria, J. P.; Palmer, A. G. *J. Magn. Reson.* **1999**, *136*, 92−101.
(28) Kojima, C.; Kainosho, M. *J. Magn. Reson.* **2000**, *143*, 417−422.
(29) Meissner, A.; Schulte-Herbruggen, T.; Sorensen, O. W. *J. Am. Chem. Soc.* **1998**, *120*, 7989−7990.
(30) Meissner, A.; Schulte-Herbruggen, T.; Sorensen, O. W. *J. Am. Chem. Soc.* **1998**, *120*, 3803−3804.
(31) Nicholas, P.; Fushman, D.; Ruchinsky, V.; Cowburn, D. *J. Magn. Reson.* **2000**, *145*, 262−275.

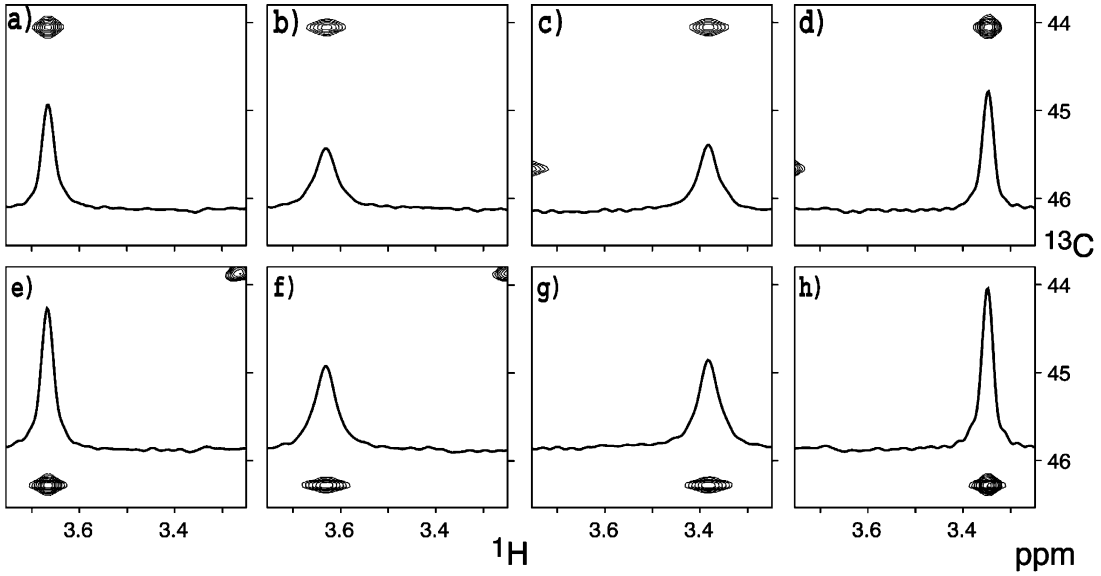

Figure 4. Experimental spectra for the eight multiplet components of Figure 1b, recorded with the pulse scheme of Figure 2a, for the Gly-41 $H^{\alpha 3}$ in GB3. The eight spectra were recorded at 10 °C, 500 MHz ^{1}H frequency, with the pulse phases listed in Table 1. Spectra a−d correspond to the C^{++} transition; e−h, to C^{--}; a and e, to H^{-+}; b and f, to H^{--}; c and g, to H^{++}, d and h, to H^{+-}. A cross section through each of the selected components is shown to highlight differences in ^{1}H line widths.

represents only ca. 2% of the selected correlation in the regular CH_2-TROSY spectrum. Use of longer delays, which still satisfy the equality $f(\tau_1, \tau_2) = g(\tau_1, \tau_2)$ (Figure 3b), can decrease the intensity of this artifact even further (Supporting Information, Figure S2). Total cancellation can be obtained for $\tau_1 = 0.50/{}^1J_{CH}$ and $\tau_2 = 0.25/{}^1J_{CH}$ but would occur at the expense of a 20% drop in sensitivity (Supporting Information, Figure S1) and an increase of other sources of artifacts. Therefore, as a compromise between sensitivity and artifact intensity, values of $\tau_1 = 0.4/{}^1J_{CH}$ and $\tau_2 = 0.24/{}^1J_{CH}$ are used. With these delays, no artifact larger than 1% is observed and the experiment still retains ≥95% of its maximum sensitivity.

High Resolution ^{1}H−^{13}C Spectra. As expected, intensities and line widths of the eight multiplet components of methylene ^{1}H−^{13}C correlation spectra vary considerably (Figure 4). The correlation between transitions C^{--} and H^{+-} exhibits the most favorable relaxation properties (Figure 4h). The longer relaxation time of H^{+-} compared to H^{-+} indicates that at the position of proton H^1, the sum of the dipolar fields corresponding to $^{13}C = |\alpha\rangle$ and $H^2 = |\beta\rangle$ decreases the "local field" of the H^1 CSA term. Similarly, the longer relaxation time of C^{--} compared to C^{++} indicates that, at the C position, the sum of the dipolar fields decreases the "local field" of the ^{13}C CSA term when both protons are in the $|\beta\rangle$ spin state. Therefore, optimal resolution is obtained when the CH_2-TROSY experiment selects this correlation.

As an example, Figure 5 compares the Gly region of such a CH_2-TROSY spectrum, recorded for the 20 kDa CaM/M13 complex, with a regular sensitivity-enhanced HSQC experiment, optimized for methylene correlations.[18,32] Comparison of ^{1}H line widths in these two spectra highlights the increased resolution.

We define a resolution enhancement factor λ_R as the ratio of the NMR signal line width measured in the HSQC and in the CH_2-TROSY spectra. The resolution enhancement factor in the ^{1}H dimension (λ_H) results from removal of the $^2J_{HH}$ splitting ($^J\lambda_H$) and selection of the slowest relaxing multiplet component ($^\Gamma\lambda_H$). To a first approximation, it is described by

$$\lambda_H = \frac{R_H + \pi \times |^2J_{HH}|}{R_H + \Gamma^{CSA,DD}_{H^1,H^1H^2} - \Gamma^{CSA,DD}_{H^1,H^1C} - \Gamma^{DD,DD}_{H^1C,H^1H^2}}$$

$$= {}^J\lambda_H \times {}^\Gamma\lambda_H = \left(1 + \frac{\pi \times |^2J_{HH}|}{R_H}\right) \times \left(1 + \frac{\Gamma^{CSA,DD}_{H^1,H^1H^2} - \Gamma^{CSA,DD}_{H^1,H^1C} - \Gamma^{DD,DD}_{H^1C,H^1H^2}}{R_H}\right)^{-1} \quad (7a)$$

where R_H is the proton autorelaxation rate: $R_H = \Gamma^{DD,DD}_{H^1C,H^1C} + \Gamma^{DD,DD}_{H^1H^2,H^1H^2} + \Gamma^{CSA,CSA}_{H^1,H^1}$. Each of the three pertinent cross-correlated rates, $\Gamma^{CSA,DD}_{H^1,H^1H^2}$, $\Gamma^{CSA,DD}_{H^1,H^1C}$, and $\Gamma^{DD,DD}_{H^1C,H^1H^2}$ can be extracted from the difference of ^{1}H line widths for suitably chosen pairs of resonances (eq 2). Analysis of spectra recorded for the CaM/M13 complex, at 35 °C and at a ^{1}H frequency of 800 MHz (data not shown), yields average values of $\Gamma^{DD,DD}_{H^1C,H^1H^2} = 27.4 \pm 3.2$ Hz, $\Gamma^{CSA,DD}_{H^1,H^1C} = 6.2 \pm 3.9$ Hz, and $\Gamma^{CSA,DD}_{H^1,H^1H^2} = -0.6 \pm 3.9$ Hz. Therefore, for moderate size proteins, the two most important factors for the line narrowing effect in the ^{1}H dimension are the dipole−dipole cross-correlated rate $\Gamma^{DD,DD}_{H^1C,H^1H^2}$ and the suppression of the $^2J_{HH}$ splitting (17−18 Hz for Gly). Whereas the absolute line narrowing caused by removal of the $^2J_{HH}$ splitting remains constant, the contribution from the cross-correlated relaxation increases with the correlation time and thereby the size of the protein. For the CaM/M13 complex, the experimentally determined resolution enhancement factor is $\lambda_H = 2.30$, with $^J\lambda_H = 1.54$ and $^\Gamma\lambda_H = 1.49$. For the tetrahedral geometry of the Gly methylene groups, substitution of our experimental value of $\Gamma^{DD,DD}_{H^1C,H^1H^2}$ into eq 5e yields $\tau_c \mathbf{S}^2 = 6.74$ ns. With a generalized order parameter $\mathbf{S}^2 = 0.8$ for Gly-C^α assumed, this corresponds to $\tau_c = 8.4$ ns, in good agreement with previous measurements.[33] No prior experimental data for the Gly-$^1H^\alpha$ chemical shielding tensor magnitude or orientation

(32) Schleucher, J.; Schwendinger, M.; Sattler, M.; Schmidt, P.; Schedletzky, O.; Glaser, S. J.; Sørensen, O. W.; Griesinger, C. *J. Biomol. NMR* **1994**, *4*, 301−306.

are available to confirm the measured cross-correlated relaxation rates, and instead we use the results from DFT calculations (see Methods). For $\tau_c S^2 = 6.74$ ns and DFT-derived ^{1}H shielding tensors, the predicted cross-correlated relaxation rates averaged over the two methylene protons ($\Gamma^{CSA,DD}_{H^1,CH^1} = +6.56$ Hz and $\Gamma^{CSA,DD}_{H^1,H^1H^2} = -0.17$ Hz) are in very good agreement with experimental results ($\Gamma^{CSA,DD}_{H^1,CH^1} = +6.2$ Hz and $\Gamma^{CSA,DD}_{H^1,H^1H^2} = -0.6$ Hz).

In the ^{13}C dimension, the resolution enhancement factor λ_C is defined as the ratio of the HSQC line width over that in CH_2-TROSY:

$$\lambda_C = \frac{R_C + \Gamma^{DD,DD}_{CH^1,CH^2}}{R_C + \Gamma^{DD,DD}_{CH^1,CH^2} + \Gamma^{CSA,DD}_{C,CH^1} + \Gamma^{CSA,DD}_{C,CH^2}} \qquad (7b)$$

where R_C is the carbon autorelaxation rate: $R_C = \Gamma^{DD,DD}_{CH^1,CH^1} + \Gamma^{DD,DD}_{CH^2,CH^2} + \Gamma^{CSA,CSA}_{C,C}$. Again assuming tetrahedral geometry and $\tau_c S^2 = 6.74$ ns, calculation of the dipole−dipole cross-correlation rate yields $\Gamma^{DD,DD}_{CH^1,CH^2} \approx -20.5$ Hz. Although this corresponds to a ca. 25% decrease in ^{13}C transverse relaxation rate compared to R_C, $\Gamma^{DD,DD}_{CH^1,CH^2}$ affects the two ^{13}C multiplet components, C^{--} and C^{++}, observed in HSQC and CH_2-TROSY identically. In contrast, the two CSA-dipole cross-correlated rates $\Gamma^{CSA,DD}_{C,CH^1}$ and $\Gamma^{CSA,DD}_{C,CH^2}$ broaden the upfield ^{13}C multiplet component and narrow the downfield, C^{--} transition, observed in the CH_2-TROSY experiment. For calmodulin Gly residues at 800 MHz, measurement of the decay rates of C^{--} and C^{++} yields $\Gamma^{CSA,DD}_{C,CH^1} + \Gamma^{CSA,DD}_{C,CH^2} = -17 \pm 5$ Hz. This corresponds to a ^{13}C resolution enhancement factor $\lambda_C = 1.4$.

Assuming $\theta^{CSA,DD}_{C,CH^1} = \theta^{CSA,DD}_{C,CH^2}$, the value of $\Delta\sigma_C \times P_2(\cos\theta^{CSA,DD}_{C,CH})$ is determined from eq 5d and the experimental $\Gamma^{CSA,DD}_{C,CH^1} + \Gamma^{CSA,DD}_{C,CH^2}$ rate. This yields $\Delta\sigma_C \times P_2(\cos\theta^{CSA,DD}_{C,CH}) = -25$ ppm, in good agreement with the experimental CSA values measured by solid-state NMR for Gly-C^α.[34]

Finally, the total resolution enhancement factor of the CH_2-TROSY over the HSQC experiment is $\lambda_R = \lambda_H \times \lambda_C = 3.2$. With the relative sign of each cross-correlated relaxation rate involved taken into account, the CH_2-TROSY experiment makes it possible to benefit from all six relaxation interference effects to reduce the decay rate of the selected multiplet component. Cross-correlated relaxation rates increase with the molecular correlation tumbling time τ_C. For the CSA values reported above, the resolution enhancement resulting from interference effects, $^\Gamma\lambda_H \times \lambda_C$, becomes larger than $^J\lambda_H$ for molecules with $S^2\tau_C$ above 5.3 ns. CSA-dipole cross-correlated relaxation increases linearly with magnetic field strength, whereas $^2J_{HH}$ coupling and, to a good approximation, dipole−dipole cross-correlated relaxation rates are field-independent. However, considering that the magnitudes of ^{1}H and ^{13}C CSA are moderate for aliphatic groups, suppression of the $^2J_{HH}$ splitting and dipole−dipole cross-correlation are the dominant factors behind the increased resolution. Therefore, the CH_2-TROSY experiment remains quite efficient at low field: a resolution enhancement factor of $\lambda_R = 2.8$ is observed for the CaM/M13 complex at 500 MHz, compared to the above-mentioned $\lambda_R = 3.2$ at 800 MHz (Table 2).

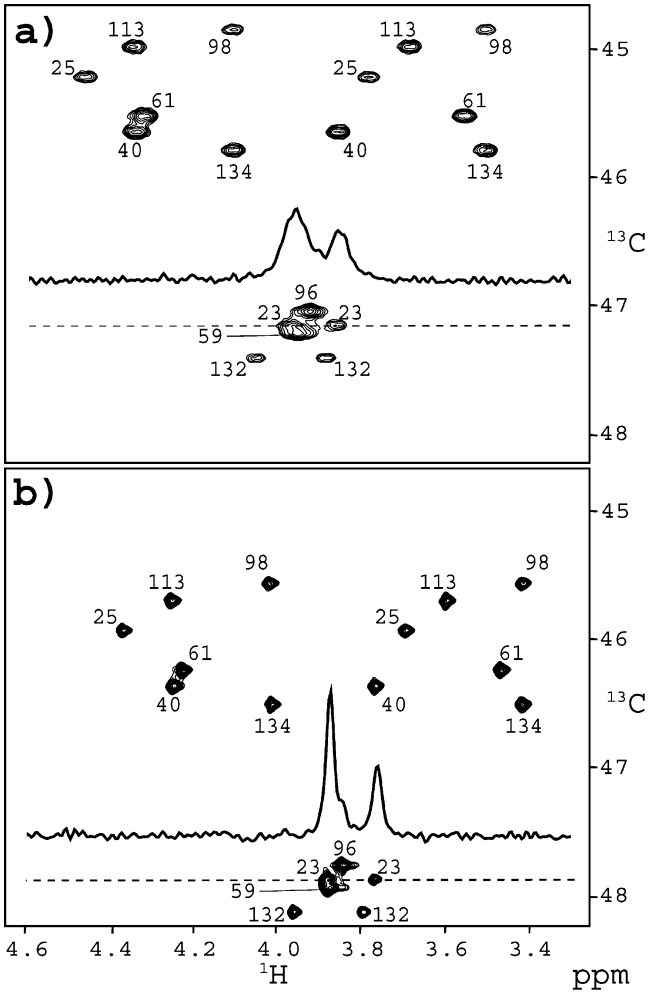

Figure 5. Comparison of (a) HSQC and (b) CH_2-TROSY spectra of Gly $C^\alpha H_2$ groups in ^{13}C-enriched calmodulin, complexed with unlabeled M13 peptide. Correlations are labeled by residue number. Both experiments were optimized for methylene detection, with the τ_1 delay of the Rance−Kay element in the HSQC experiment adjusted to $1/(8^1J_{CH})$.[32] Spectra were recorded at 800 MHz, 35 °C, with a relaxation delay of 2.5 s and total measuring times of 2.3 h each. Identical acquisition and processing parameters were used: time domain matrices of 192* × 640* data points, with acquisition times of 96 ms (t_1) and 80 ms (t_2), no apodization of the time domain data. Spectra are plotted at identical contour levels, and correlations are labeled by residue number. Inset cross sections, taken at the position of the dashed lines, correspond to Gly-23. The average resolution enhancement obtained with CH_2-TROSY is $\lambda_R = 3.2$, while sensitivity is increased by the factor $\lambda_S = 2$.

Table 2. Average Observed Gly $C^\alpha H_2$ Resolution and Sensitivity Enhancement Factors in a Calmodulin/Peptide Complex[a]

B_0 (T)[b]	λ_H[c]	λ_C[c]	λ_R[c]	λ_S[c]
11.75	2.3	1.2	2.8	1.6
18.8	2.3	1.4	3.2	2.0

[a] Data at 35 °C for a (^{13}C, ^{15}N)-labeled sample of the 20 kDa CaM/M13 complex in D_2O. [b] The recycle delay, optimized for maximum sensitivity, is 1.8 s at 11.75 T and 2.5 s at 18.8 T. [c] The resolution enhancement factors λ_H and λ_C are defined as the ratios of the ^{1}H (λ_H) and the ^{13}C line widths in the regular HSQC and CH_2-TROSY spectra. The total resolution enhancement factor, λ_R, equals the product of λ_H and λ_C. The sensitivity enhancement factor, λ_S, is the ratio of the intensity in the CH_2-TROSY and regular HSQC spectra, recorded with identical acquisition and processing parameters.

Sensitivity Enhancement. Compared to the regular HSQC experiment only one-half of the initial ^{1}H polarization is retained after the S^3E filter ($\lambda_{S^3E} = 0.5$). This loss is partially compensated

(33) Lee, A. L.; Sharp, K. A.; Kranz, J. K.; Song, X. J.; Wand, A. J. *Biochemistry* **2002**, *41*, 13814−13825.
(34) Yao, X. L.; Hong, M. *J. Am. Chem. Soc.* **2002**, *124*, 2730−2738.

by the addition of the ^{13}C Boltzmann polarization, which contributes to the detected signal in the CH_2-TROSY experiment, as discussed previously. At the end of the INEPT element (time point *a*, Figure 2a) the signal intensity is described by the following: $I(\delta) = M_H(\delta) \times [2C_xH_z^1 + 2C_xH_z^2] + M_C(\delta) \times [C_x]$, where $M_X(\delta)$ is the initial Boltzmann magnetization for nucleus X, using a recycling delay, δ. $I(\delta)$ can be decomposed in terms of single-transition operators C^{PQ} (eq 3):

$$I(\delta) = C^{--}\left(\frac{M_C(\delta)}{4} + \frac{M_H(\delta)}{2}\right) + C^{++}\left(\frac{M_C(\delta)}{4} - \frac{M_H(\delta)}{2}\right) + \frac{M_C(\delta)}{4}(C^{+-}+C^{-+}) \quad (8)$$

Only C^{--} is selected in the CH_2-TROSY experiment. Because M_X is directly proportional to the gyromagnetic ratio, γ_X, of X ($\gamma_H/\gamma_C \approx 4$; *i.e.*, $M_H/M_C \approx 4$), eq 8 indicates that a 12.5% signal increase is expected when the ^{13}C Boltzmann magnetization is added. A larger sensitivity gain is expected under nonequilibrium, steady-state conditions for the case where $T_1(^1H) > T_1(^{13}C)$.[4,24]

The dependence of signal contributions resulting from ^1H and ^{13}C steady-state polarization as a function of the recycle delay, δ, has been measured for the calmodulin Gly residues at a 18.8-T (800 MHz ^1H frequency) magnetic field strength (Supporting Information, Figure S3). Optimal signal-to-noise per unit of measuring time is obtained for $\delta \approx 2.5$ s. At this interscan delay, the ^{13}C Boltzmann magnetization corresponds to a signal increase of 33% over the case where only the magnetization transferred from ^1H is selected. In practice, shorter interscan delay times are frequently used to complete all required phase cycling steps in a finite amount of available measurement time. For a typical $\delta \approx 1$ s duration, the ^{13}C Boltzmann component increases the signal by 50%; i.e., the total amount of observed ^1H magnetization becomes 75% of that in a regular HSQC experiment.

The line narrowing effect resulting from cross-correlated relaxation in both ^1H and ^{13}C dimensions also contributes to increased intensity of the detected signal in the CH_2-TROSY experiment. However, if the acquisition time in the ^{13}C dimension were adjusted to a fixed multiple of the effective ^{13}C magnetization decay constant, the slower decay of ^{13}C magnetization has a negligible effect on the sensitivity of the experiment per unit of measuring time. In contrast, in the directly detected ^1H dimension, where longer sampling does not increase the total time of the experiment, sensitivity per unit of measuring time increases with the square root of the obtained resolution enhancement factor, again assuming that the acquisition time equals a fixed multiple of the decay constant in the two experiments. In practice, sensitivity comparisons of regular and TROSY type experiments are commonly carried out under conditions where identical sampling times are used for the regular and the TROSY-type experiments,[2,35] a comparison which increases the apparent sensitivity in the TROSY-type experiment, but which obviates calculation of the precise, residue-dependent timing parameters needed for optimizing each experiment. For simplicity, we therefore adhere to this common practice and compare data sets that have identical sampling durations in both ^1H and ^{13}C dimensions and process the spectra without any apodization of the time domain data.

Under these conditions, the expected sensitivity enhancement factor coming from favorable relaxation properties of the CH_2-TROSY experiment equals $2 \times \lambda_C \times {}^\Gamma\lambda_H$, where λ_C and ${}^\Gamma\lambda_H$ are defined in eq 7, and where the factor 2 is due to the suppression of the $^2J_{HH}$ splitting, assuming $^2J_{HH}$ is resolved in the HSQC spectrum. As discussed above, experimentally we find $\lambda_C = 1.4$ and ${}^\Gamma\lambda_H = 1.49$ for the Gly-$C^\alpha H_2$ spin system at $B_0 = 18.8$ T. However, an additional factor, λ_T, needs to be defined to account for the reduced transfer efficiency of the CH_2-S^3CT transfer relative to a methylene-optimized, sensitivity-enhanced Rance−Kay element. This factor depends on the delays τ_1 and τ_2 (Supporting Information Figure S1) and has a maximum for $\tau_1 = 0.34/^1J_{CH}$ and $\tau_2 = 0.23/^1J_{CH}$ ($\lambda_T = 0.85$). With all of the described effects taken into account (^{13}C spin state selection, use of ^{13}C Boltzmann polarization, cross-correlated relaxation, proton−proton decoupling enhancements, and transfer efficiency), the total sensitivity enhancement is then given by

$$\lambda_S = \lambda_{S^3E} \times \left(\frac{M_C(\delta) + M_H(\delta)}{M_H(\delta)}\right) \times 2 \times \lambda_C \times {}^\Gamma\lambda_H \times \lambda_T \quad (9)$$

yielding a value of $\lambda_S = 2.2$, in good agreement with a value of 2.0, observed experimentally at 800 MHz (Table 2). The 10% discrepancy between predicted and experimentally determined sensitivity enhancements is likely to result from two factors neglected in the above calculation: the effect of relaxation during the very short S^3E filtering delay and partial overlap of the two ^1H doublet components in the reference HSQC spectrum. This partial overlap increases the apparent HSQC intensity and, therefore, reduces the observed gain of the CH_2-TROSY experiment. When it is considered that much of the gain in resolution and sensitivity results from dipole−dipole cross correlation effects, which are independent of magnetic field strength, the CH_2-TROSY experiment remains advantageous across the entire range of commonly used magnetic field strengths. Indeed, a sensitivity enhancement factor of $\lambda_S = 1.6$ was observed for the CaM/M13 sample at 500 MHz, only 20% less compared to the gain observed at 800 MHz.

Effect of Nongeminal $^1H-^1H$ Interactions. Above, discussions focused on an isolated three-spin system, exemplified through the study of Gly methylene groups. However, the experiment is directly applicable to all methylene sites in macromolecules. For such nonisolated methylenes, remote $^1H-^1H$ interactions need to be taken into account when evaluating the merits of the CH_2-TROSY experiment. Both passive scalar interaction, $^3J_{HH}$, and dipolar $^1H-^1H$ relaxation with the additional protons will broaden the ^1H signal, whereas the effect of the additional protons on the ^{13}C decay will be negligible compared to that of its directly bonded protons. For the methylene protons, the difference in ^1H line width between the CH_2-TROSY and regular HSQC experiments is not affected by the additional presence of neighboring protons, but the relative resolution and sensitivity gain decrease as the remote protons broaden the ^1H line width in both types of experiments by the same amount.

The effect of protons in the vicinity of a methylene group can be described by adding the following terms to both the

(35) Tugarinov, V.; Kay, L. E. *J. Mol. Biol.* **2003**, *327*, 1121−1133.

numerator and denominator of λ_H (eq 7a): $\Sigma_{j\neq1,2}\,\pi \times {}^3J_{H^iH^j} + \Sigma_{j\neq1,2}\,\Gamma^{DD,DD}_{H^iHj,H^iHj}$, where H^i ($i = 1,2$) denotes one of the methylene protons. For macromolecules, such line broadening often will cause the geminal $^2J_{HH}$ coupling to be unresolved in the reference HSQC spectrum. Removal of the $^2J_{HH}$ coupling contribution to the ^{1}H line shape will narrow the resonance in the CH_2-TROSY spectrum but will appear less pronounced than for the case of isolated methylenes. Also, the additional ^{1}H−^{1}H dipolar interactions increase the effective ^{1}H longitudinal relaxation rate of methylene protons, without significantly affecting the relaxation rate of ^{13}C, thereby reducing the fractional contribution of the Boltzmann ^{13}C polarization.

To evaluate the enhancement offered by the CH_2-TROSY experiment for nonisolated methylene groups experimentally, we recorded CH_2-TROSY and regular ^{1}H−^{13}C HSQC spectra for GB3 at 800 MHz and 10 °C. The GB3 protein (56 residues) is much smaller than calmodulin and yields resolved correlations for most of its methylene resonances, in both the CH_2-TROSY and HSQC spectra (Supporting Information, Figure S4). The spectra can be recorded either in the constant-time (CT) mode (using a CT ^{13}C evolution period of $1/{}^1J_{CC} \approx 28$ ms)[36] or in the regular manner. If the CH_2-TROSY spectrum is recorded in the CT mode, ${}^nJ_{CH}$ couplings ($n \geq 2$) are not decoupled and cause some attenuation at the end of the CT evolution period: for example, ${}^nJ_{CH} = 7$ Hz results in a 20% loss of magnetization. On the other hand, as is the case for 3D ^{15}N TROSY-based experiments,[37] the favorable ^{13}C relaxation properties apply for the full duration of the CT period, T, whereas in the regular CT-HSQC favorable relaxation applies to the two multiplet components for durations of $T - t_1/2$ and $t_1/2$. This changes the intensity of the CH_2-TROSY signal by a factor of $2(\Gamma^{CSA,DD}_{C,CH^1} + \Gamma^{CSA,DD}_{C,CH^2}) \times T/(1 - \exp -2(\Gamma^{CSA,DD}_{C,CH^1} + \Gamma^{CSA,DD}_{C,CH^2})T)$ relative to that in the HSQC experiment. In the CT mode, this factor should substitute for λ_C in eq 9 when calculating the sensitivity enhancement factor, λ_S. This λ_S factor increases with the size of the molecule, and its magnitude becomes larger than the enhancement obtained for regular, non-CT acquisition mode (eq 7b) when $\mathbf{S}^2\tau_C \geq 5.7$ ns, assuming a regular CT duration of $T = 28$ ms. For side chain methylene carbons, we find that the intensity ratio observed in CH_2-TROSY versus HSQC spectra is also strongly influenced by the amplitude of internal dynamics of the methylene group, with more internal motion resulting in a smaller value of λ_S.[38] In constant-time experiments, improved spectral appearance therefore mainly results from the line narrowing obtained in the ^{1}H dimension. This latter effect depends strongly on the number of protons geminal to the methylene carbon in question. C^β methylenes of Cys, Ser, Asp, Asn, Phe, Tyr, Trp, and His each have only a single proton (H^α) that is J-coupled to H^β. For these residues, the gain in ^{1}H resolution is, on average, $\lambda_H = 1.7$ (Table 3). Smaller gains are obtained for C^β methylenes of Met, Glu, Gln, Arg, and Lys residues (Table 3), where three vicinal protons have $^3J_{HH}$ and dipolar interactions with H^β.

When comparing C_2' to C_5' methylene groups in DNA, we also find smaller enhancements in resolution and sensitivity: $\lambda_H = 1.6$ vs 1.9 and $\lambda_S = 1.0$ vs 1.3 (Table 3). The disappearance of a sensitivity gain is again consistent with the topology of the ^{1}H−^{1}H network: H_5'/H_5'' are only coupled to H_4', whereas H_2'/H_2'' protons are J-coupled to both H_1' and H_3'. Nevertheless, as will be demonstrated below, even this moderate (60−90%) gain in resolution can considerably enhance spectral appearance.

Table 3. Resolution and Sensitivity Enhancement Factors for Methylene Sites in Proteins and DNA[a]

CH_2 type	G^b	C, S, D, N, F, Y, W, H[b]	M, Q, E, K, R[b]	C_2'[c]	C_5'[c]
λ_H	2.3	1.7	1.4	1.6	1.9
λ_S	1.7	1.0	0.8	1.0	1.3

[a] Data recorded at 800 MHz, using the pulse sequence of Figure 2a for samples of (^{13}C, ^{15}N)-enriched GB3 (T = 10 °C), and using the pulse sequence of Figure 2b for a 19-basepair DNA oligomer (T = 35 °C), both in D_2O. The resolution enhancement factor, λ_H, corresponds to the average ^{1}H line width in the regular HSQC experiment divided by that in the CH_2-TROSY experiment. The sensitivity enhancement factor, λ_S, is the ratio of the intensity in the CH_2-TROSY spectrum divided by that in the regular HSQC spectrum, recorded with identical acquisition and processing parameters. [b] One-letter amino acid residue type. Numbers listed apply for $C^\beta H_2$. On average, the optimal CH_2-TROSY recycle delay was found to be ca. 1 s for Gly-C^α and ca. 0.5 s for side chain CH_2. [c] Methylene groups in the DNA oligomer. The optimal CH_2-TROSY recycle delay for CH_2 groups in DNA was 0.8 s.

The smaller enhancements observed in the CH_2-TROSY experiment when applied to groups embedded in an environment rich in protons is similar to that observed in other TROSY methods, such as those employed for enhancing signals of ^{15}N−^{1}H pairs[1] or ^{13}C−$^1H_3$ groups.[6] In these latter experiments, signal enhancement is considerably enhanced when neighboring protons are replaced by deuterons. For the CH_2-TROSY experiment described here, in the absence of deuteration, a dense proton environment may lead to a small loss in sensitivity compared to a standard, methylene-optimized HSQC experiment. However, the gain in ^{1}H resolution remains quite pronounced, making the experiment useful for unravelling the typically crowded methylene region of protein and nucleic acid spectra.

Application to Sequential Assignment of Nucleic Acids. The CH_2-TROSY enhancement can readily be incorporated in the wide range of commonly used 3D experiments. Here, its benefit is illustrated for the 3D ^{13}C-separated NOESY experiment, applied to DNA.

In nucleic acids, NOE interactions between adjacent nucleotides constitute the mainstay of sequential assignment. For ^{13}C-enriched RNA, the conventional TROSY approach has been shown to improve substantially the ^{13}C resolution of base carbons, benefiting the 3D ^{13}C-separated NOESY experiment for observation of sequential base $H_{6/8}$ to H_1' NOEs.[4] However, the shortest distances between sequential nucleotides in a standard duplex helix involve protons in the C_2' and C_5' positions.[39] These NOEs are often difficult to analyze because of spectral overlap, especially in the C_5' region. Below, we demonstrate that incorporation of the CH_2-TROSY element considerably improves spectral resolution, thereby permitting the study of sequential NOEs involving H_2'/H_2'' and H_5'/H_5'' protons.

Table 3 reports the resolution and sensitivity enhancement factors for the C_2' and C_5' methylene groups in a 19-base-pair DNA fragment,[12] when comparing the 2D version of the CH_2-TROSY experiment of Figure 2b with that of the analogous methylene-optimized HSQC experiment. Comparison of the C_5'

(36) Vuister, G. W.; Bax, A. *J. Magn. Reson.* **1992**, *98*, 428−435.
(37) Salzmann, M.; Pervushin, K.; Wider, G.; Senn, H.; Wuthrich, K. *Proc. Natl. Acad. Sci. U.S.A.* **1998**, *95*, 13585−13590.
(38) Yang, D. W.; Mittermaier, A.; Mok, Y. K.; Kay, L. E. *J. Mol. Biol.* **1998**, *276*, 939−954.
(39) Wijmenga, S. S.; van Buuren, B. N. M. *Prog. Nucl. Magn. Reson. Spectrosc.* **1998**, *32*, 287−387.

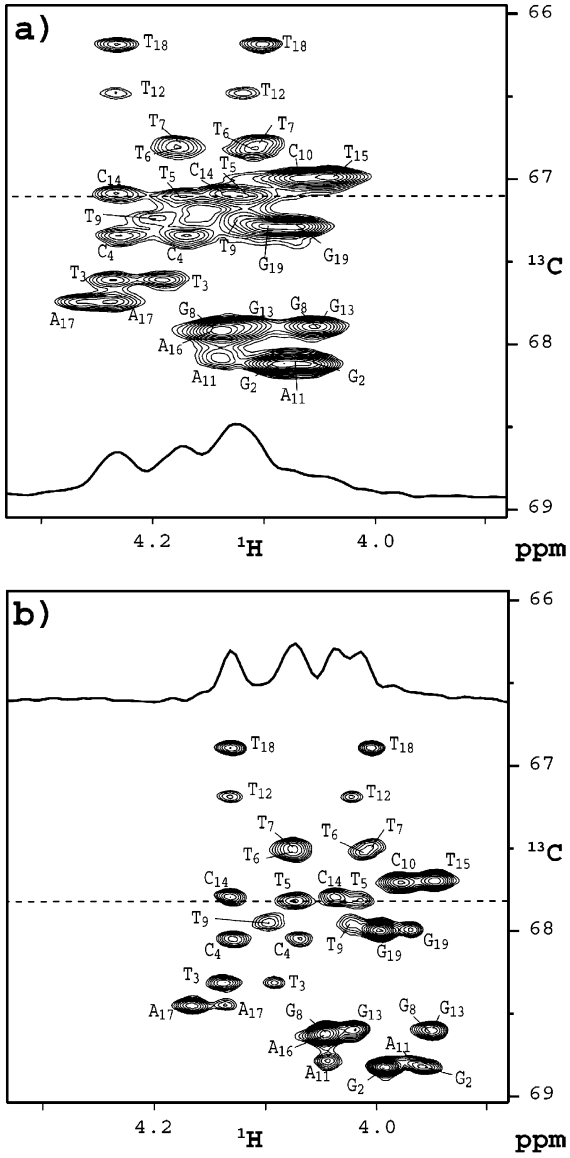

Figure 6. Comparison of (a) sensitivity-enhanced HSQC and (b) CH_2-TROSY spectra of the C_5' region of a 19-base-pair DNA oligomer for which one strand was uniformly enriched in ^{13}C. Spectra were recorded at 800 MHz, 35 °C, with measuring times of 1.2 h per spectrum. Spectra result from identical time domain matrices, consisting of 200* × 512* data points, recorded with acquisition times of 96 ms (t_1) and 64 ms (t_2). Data were processed identically, without apodization of the time domain data. Spectra are plotted at the same contour levels. Cross sections show the C_5' correlations of T5 and C14.

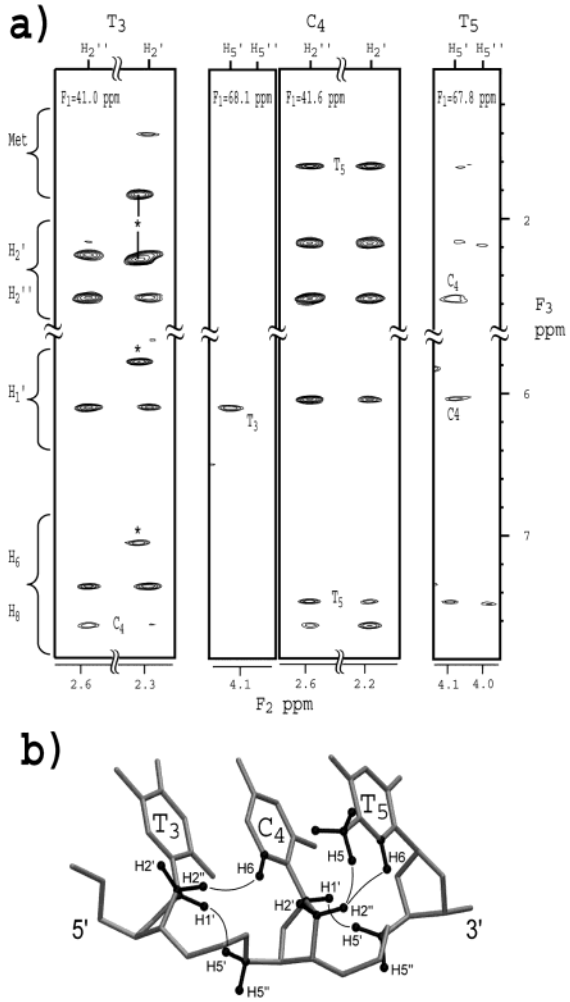

Figure 7. Sequential connectivity involving methylene protons in a DNA oligomer. (a) Strips taken for nucleotides T3, C4, and T5 from the 3D ^{13}C-separated CH_2-TROSY-NOESY spectrum, recorded on the 19-base-pair DNA duplex with the pulse scheme of Figure 2b. The spectrum was recorded at 800 MHz, 35 °C, 250 ms NOE mixing time, and a total measuring time of 48 h. The time domain matrix consisted of 122* × 55* × 512* data points, with acquisition times of 55 ms (t_1), 50 ms (t_2), and 64 ms (t_3). Only sequential NOEs are labeled in the figure. Due to partial overlap, the T3-C_2' strip also contains correlations for T18, marked by asterisks. (b) Summary of the observed sequential connectivities for T3-C4-T5, modeled in B-form helical geometry.

regions of the 2D CH_2-TROSY and HSQC spectra (Figure 6) confirms a considerable enhancement in spectral resolution, resulting in a nearly 2-fold increase in the number of resolved resonances.

In B-form DNA, the two shortest distances between sequential nucleotides i and $i + 1$ involve pairs $H_2''(i)/H_{6/8}(i + 1)$ and $H_1'(i)/H_5''(i + 1)$. We demonstrate that the latter interaction can be readily observed when the CH_2-TROSY element is incorporated in the 3D ^{13}C-separated NOE experiment. In our implementation (Figure 2b), the TROSY element is placed before the NOE mixing period, such that the enhancement resulting from the ^{13}C Boltzmann magnetization is retained and the relatively well dispersed H_1' and $H_{8/6}$ resonances are observed during the detection period, t_3. When it is considered that $^{13}C_2'$ and $^{13}C_5'$ chemical shifts are well separated from $^{13}C_1'$, $^{13}C_3'$, and $^{13}C_4'$, band-selective adiabatic homonuclear decoupling was used to eliminate the large one-bond $^1J_{CC}$ couplings ($^1J_{CC} \approx 40$ Hz).[40]

Figure 7 shows small regions of strips taken through the 3D CH_2-TROSY-NOESY spectrum of the 19-base-pair DNA oligomer, highlighting some of the NOE connectivities observable for C_2' and C_5' methylene protons. Because of the absence of homonuclear $^{13}C-^{13}C$ and geminal $^1H-^1H$ J splittings, as well as the slower transverse relaxation resulting from the CH_2-TROSY element, high spectral resolution is obtained in both the indirect ^{13}C (F_1) and ^{1}H (F_2) dimensions. This, for example, yields resolved correlations for the C_2' protons of nucleotide T3, which overlap with T18 in the regular HSQC-NOESY spectrum (data not shown). As expected, sequential NOEs among $H_2''(T3)/H_6(C4)$, $H_2''(C4)/H_6(T5)$, $H_5''(C4)/H_1'(T3)$, and $H_5''(T5)/H_1'(C4)$ are clearly visible and readily permit the sequential assignment to be made. Relatively intense intranucleotide NOE cross-peaks are also visible between H_2' and the

base H_6 proton, with a weaker correlation between H_2'' and H_6 resulting from spin diffusion via H_2' during the relatively long NOE mixing time (250 ms). For this mixing time, intranucleotide correlations between H_5''/H_5' and H_1' are absent and only the H_5''/H_1' sequential connectivity is observed. Therefore, the 3D ^{13}C-separated CH_2-TROSY-NOESY experiment offers two separate pathways for sequential assignment, which complement each other in cases of ambiguities resulting from spectral overlap.

Concluding Remarks

Detailed analysis of NMR signals involving the abundant methylene protons in macromolecules is frequently hampered by severe spectral crowding and rapid transverse relaxation. This problem provided the impetus behind a powerful but labor-intensive new isotope labeling procedure, known as SAIL,[41] where one of each pair of methylene hydrogens is substituted stereospecifically by deuterium. Instead, the CH_2-TROSY approach is aimed at the more general case where uniform ^{13}C enrichment, but no selective deuteration, is used. The CH_2-TROSY experiment yields considerable enhancement in resolution in both the ^1H and ^{13}C dimensions and can offer a modest increase in sensitivity too. As most of the gain in resolution results from dipole−dipole cross-correlation and from removal of the $^2J_{HH}$ splitting, which are both independent of magnetic field strength, the approach is beneficial over the entire range of commonly used magnetic field strengths.

The CH_2-TROSY element can be incorporated in a wide variety of NMR experiments, thereby potentially facilitating both resonance assignment and the extraction of structural and dynamic parameters involving methylene groups. The spectral enhancement resulting from the CH_2-TROSY element is largest when applied to isolated methylene groups, such as those found in Gly residues. These are often located in turn regions in proteins, whose precise geometry is frequently difficult to identify from the low number of restraints that typically can be extracted for these residues from conventional spectra. When the molecule is weakly aligned relative to the magnetic field, the ability to separately observe any of the methylene $^{13}C-^1H$ multiplet components also permits measurement of all three dipolar couplings for such a group. Besides the important structural information this offers, we currently are also investigating the application of the measurement of three independent dipolar couplings in the plane of the methylene moiety to characterize its dynamic properties.

Acknowledgment. We thank F. Delaglio for writing the special processing macro required for the Fourier transform of the 3D TROSY-NOESY and H. Kovacs for help in implementing homonuclear ^{13}C adiabatic decoupling. J.B. is supported by an HFSP fellowship; E.M., by an ARC fellowship; D.C.W., by a PRAT fellowship; and D.L.B., by an NSERC fellowship. This work was supported in part by the Intramural AIDS Targeted Antiviral Program of the Office of the Director of the National Institutes of Health.

Supporting Information Available: Four figures showing the following: CH_2-TROSY transfer efficiency as a function of transfer delays τ_1 and τ_2; the relative intensity of spurious peak corresponding to transition C^{-+} and C^{+-}; experimental signal-to-noise as a function of interscan delay in CH_2-TROSY; comparison of side chain methylene regions of GB3, recorded with CH_2-TROSY and regular HSQC. This material is available free of charge via the Internet at http://pubs.acs.org.

JA047904V

(40) Brutscher, B.; Boisbouvier, J.; Kupce, E.; Tisne, C.; Dardel, F.; Marion, D.; Simorre, J. P. *J. Biomol. NMR* **2001**, *19*, 141−151.
(41) Torizawa, T.; Terauchi, T.; Kainosho, M. *Seikagaku* **2002**, *74*, 1279−1284.